



# Lawrence Berkeley Laboratory

UNIVERSITY OF CALIFORNIA

## Materials & Molecular Research Division

To be published in Discussions of the Faraday Society #71,  
"High Resolution Spectroscopy", 1981

LASER INDUCED FLUORESCENCE OF TRAPPED MOLECULAR IONS:  
THE  $CH^+ A^1\Pi \leftarrow X^1\Sigma^+$  SYSTEM

Fred J. Grieman, Bruce H. Mahan, Anthony O'Keefe,  
and John S. Winn

September 1980

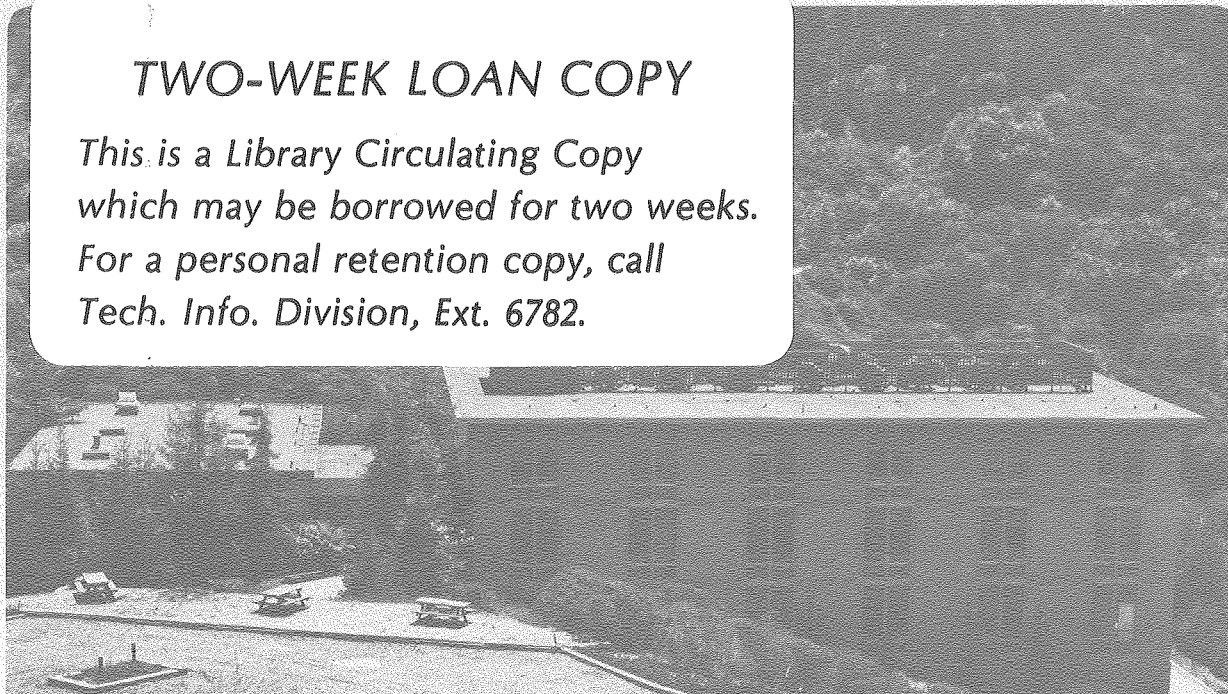
RECEIVED  
LAWRENCE  
BERKELEY LABORATORY

NOV 6 1980

LIBRARY AND  
DOCUMENTS SECTION

### TWO-WEEK LOAN COPY

*This is a Library Circulating Copy  
which may be borrowed for two weeks.  
For a personal retention copy, call  
Tech. Info. Division, Ext. 6782.*



LBL-11534 c.2

## DISCLAIMER

This document was prepared as an account of work sponsored by the United States Government. While this document is believed to contain correct information, neither the United States Government nor any agency thereof, nor the Regents of the University of California, nor any of their employees, makes any warranty, express or implied, or assumes any legal responsibility for the accuracy, completeness, or usefulness of any information, apparatus, product, or process disclosed, or represents that its use would not infringe privately owned rights. Reference herein to any specific commercial product, process, or service by its trade name, trademark, manufacturer, or otherwise, does not necessarily constitute or imply its endorsement, recommendation, or favoring by the United States Government or any agency thereof, or the Regents of the University of California. The views and opinions of authors expressed herein do not necessarily state or reflect those of the United States Government or any agency thereof or the Regents of the University of California.

Laser Induced Fluorescence of Trapped Molecular Ions:

The  $\text{CH}^+ \text{A}^1\Pi \leftarrow \text{X}^1\Sigma^+$  System

\* Fred J. Grieman, Bruce H. Mahan, Anthony O'Keefe and John S. Winn

Department of Chemistry, University of California  
and

Materials and Molecular Research Division  
Lawrence Berkeley Laboratory  
Berkeley, California 94720

---

\* Present address: Department of Physics  
University of Oregon  
Eugene, OR 97403

## ABSTRACT

The  $\text{CH}^+$  and  $\text{CD}^+$   $\text{A}^1\Pi \leftarrow \text{X}^1\Sigma^+$  absorption spectra have been obtained by laser excitation of these fragment ions. The ions are contained in a mass-selective quadrupole ion trap under collision free conditions. The spectra therefore reflect the nascent internal energy distributions of the ions, which were produced by electron impact on  $\text{CH}_4$  ( $\text{CD}_4$ ) or  $\text{C}_2\text{H}_2$  ( $\text{C}_2\text{D}_2$ ). Both parent gases gave virtually identical spectra; large rotational and vibrational excitation was observed. The equipment was also capable of measuring the radiative lifetime of  $\text{CH}^+$  ( $\text{CD}^+$ )  $\text{A}^1\Pi$  ( $v=0$ ), and the measured value, 815 nsec, is found to be in good agreement with theoretical calculations of this quantity.

## INTRODUCTION

The  $\text{CH}^+$  radical has been the subject of numerous experimental and theoretical investigations since its spectroscopic identification by Douglas and Herzberg.<sup>1</sup> This small, reactive radical is of great importance in combustion reactions and atmospheric chemistry and is believed to play a fundamental role in the creation of many small molecules within the interstellar clouds. The first spectroscopic observation of this ion was made in spectra of the interstellar medium,<sup>2</sup> the observed transitions belonging to the  $\text{CH}^+ \text{A}^1\Pi \leftarrow \text{X}^1\Sigma^+$  system.

Klemperer and Solomon<sup>3</sup> have made a detailed analysis of the interstellar processes involving  $\text{CH}^+$  which are believed to have a significant effect upon the molecular composition of interstellar clouds. This ion is believed to be important in the formation of CH, CO, CN and several other molecular species. The chemistry involved in these processes is intimately related to the relative concentrations of the species involved. These concentrations must be inferred from an analysis of observed line strengths of stellar spectra and known or calculated oscillator strengths. In the case of  $\text{CH}^+$ , the uncertainty in the radiative lifetime for the  $\text{A} \rightarrow \text{X}$  transition manifests itself in a large uncertainty in stellar abundance and, in turn, to confusion over the relative importance of various chemical reactions occurring in the interstellar medium. This uncertainty arises not from the lack of experimental and theoretical study, but from the failure of such study to reach a consistent result.

Until recently<sup>4</sup> the only experimental method useful in the high resolution study of molecular fragment ions has been emission spectroscopy. While this technique is a powerful one, radiative transition

rates obtained in this manner are subject to errors which are often difficult to identify or estimate. The problems arise from the complicated nature of the excitation process. One often creates many highly excited states which may cascade down to the level of interest leading to a distortion in the measured decay rate. The  $A^1\Pi \rightarrow X^1\Sigma^+$  radiative decay rate has been the subject of five experimental studies<sup>5-9</sup> each resulting in apparently single exponential decay curves corresponding to radiative lifetimes ranging from 70 nsec to 630 nsec for the (0,0) band. All of the experimental values also appeared to contradict the theoretical estimate of Yoshimine et al.,<sup>10</sup>  $\tau_0 \approx 800$  nsec.

We have developed a technique with which we obtain the laser induced fluorescence spectra of ions confined to a small (1 cc) spatial region within a three dimensional radio frequency quadrupole trap. This trap is similar to the arrangement described by Dawson,<sup>11</sup> and it allows us to store large numbers of ions for time periods which are limited only by collisions with background neutral gas molecules. Using the Langevin estimate for the ion-neutral collision rate, we find that for a neutral gas background pressure of  $10^{-5}$  Torr, each ion will experience one collision per msec. This is expected to be an upper bound for the actual collision rate and, in practice, we find little difficulty in storing reactive species, such as  $\text{CH}^+$ , for periods of 5 to 10 msec in this pressure range. Because the trap can store ions for such long periods this arrangement provides an attractive possibility for the study of radiative decay rates. Ions which are in the ground (or an optically metastable) electronic state can be excited with a brief laser pulse and the resulting fluorescence monitored as a function of time. The observed decay rate provides an unambiguous measurement of the upper levels' radiative lifetime.

The experimental system described here is capable of storing ions in a mass selective mode, thus removing any doubt, in most cases, as to the identity of the ion under investigation. The degree of mass differentiation is variable, and in the high resolution mode of operation ions differing by only 1 amu can be resolved. Such resolving power is important in any studies involving hydrogen-containing ions.

We present here a detailed description of our experimental apparatus and results on the  $\text{CH}^+$  and  $\text{CD}^+$   $A^1\Pi - X^1\Sigma^+$  system.

#### EXPERIMENTAL

The ion trap used in this study was one of cylindrical geometry which has been described in detail elsewhere.<sup>12</sup> This configuration was selected instead of the more general hyperbolic geometry in an effort to minimize electric field distortion introduced by the presence of laser beam entrance and exit holes in the electrode. The trap consists of a cylindrical center electrode and two flat end electrodes, positioned at opposite ends of the cylinder. The general configuration is illustrated in Fig. 1. The details of trap operation will be briefly outlined here. Further details may be obtained in the references already cited.

The principles of operation are an extension to three dimensions of those involved in a conventional quadrupole ion lens. Application of an R.F. voltage to the center electrode creates a pseudo-potential in which ions are trapped regardless of their charge to mass ratio. By floating the applied R.F. voltage at some D.C. bias level a selectivity in the charge to mass ratios which are confined in the potential well is introduced. The degree of selectivity is determined by the relative

magnitudes of the D.C. and R.F. voltages. By varying the R.F. amplitude, at a fixed D.C. to R.F. ratio, the mass selection window may be shifted to different values, with ions of larger masses being trapped for greater applied voltages.

Given the general design of the trap, the depth of the pseudo-potential well can be expressed as<sup>13</sup>

$$\bar{D} = \frac{eV^2}{4A_0^2 Mf^2} = \frac{6.109 \times 10^{-3} V^2 \text{ volts}}{Z_0^2 Mf^2 \text{ cm amu MHz}}$$

Here  $\bar{D}$  is calculated in volts,  $V$  is the maximum A.C. voltage between the electrodes,  $Z_0$  is half the minimum separation of the cap electrodes,  $M$  is the ion mass in amu, and  $f$  is the applied field frequency in megahertz. In the present study the values for these parameters are  $Z_0 = 1$ ,  $V \approx 200$ ,  $M = 13$  and  $f = 1$ , and the corresponding well depth is 19 volts. The well depth determines the number of ions which can be trapped, since the trap reaches its maximum capacity when the space charge potential cancels the trapping potential. At this point the maximum concentration of ions is given by<sup>13</sup>

$$n_{\text{max}} \left( \frac{\text{ions}}{\text{cc}} \right) = \frac{1.66 \times 10^{6\bar{D}}}{Z_0^2}.$$

Thus for a well depth of 19 volts we find that  $3 \times 10^7$  ions can be trapped. When the instrument is operated as a mass spectrometer the total capacity of the trap is smaller by a factor which is difficult to calculate; however, the variation of laser induced fluorescence intensity with increasing mass selectivity for ions such as  $N_2^+$  and  $CO^+$  indicates an ion density drop by a factor between 2 and 5. In the present study, the fragmentation pattern of  $CH_4$  necessitated the use of bias conditions capable of discriminating between ions differing by only 1 amu.

Ions are created within the trap by electron impact ionization of a selected background neutral gas which is introduced into the vacuum chamber through a variable leak valve and which is maintained at a pressure of from  $10^{-6}$  to  $10^{-5}$  Torr. Fragment  $\text{CH}^+$  was generated by the electron impact dissociation of  $\text{CH}_4$  (approx. 2-3% of the total ion products) and  $\text{CD}^+$  was produced analogously from  $\text{CD}_4$ . The trap has been found to attain maximum ion density after a 2 msec electron pulse from an electron gun producing an average  $e^-$  beam current of 10  $\mu\text{amp}$ .

The electron gun consists of a resistively heated 1 cm strip of 0.25 mm diameter thoriated tungsten wire mounted on a ceramic base and enclosed within a metal shield which is floated at the center electrode potential. This shielding serves to reduce scattered light emitted from the hot filament. One of the focusing lenses also serves as an electron shutter through the application of a high voltage pulse to the lens element.

While the trapping potential operates continuously, the remainder of the experiment is operated in a pulsed mode at a repetition rate of 10-40 Hz. The remainder of the experiment is then most easily described by considering one experimental cycle which consists primarily of three parts: ion creation and confinement, excitation of the ions, and fluorescence signal detection.

The experiment begins with the initiation of the electron beam which creates ions for a period of several milliseconds. The electron gun is then gated off and a delay period of several hundred microseconds ensues. During these times any necessary mass selection of the ions is allowed to stabilize, and any excited electronic states which have been created are permitted to relax radiatively. Radiative relaxation of excited

vibrational levels within stable electronic states is expected to be slow on the time scale of an experimental cycle. The pressure range in which we operate allows little or no collisional relaxation. After the delay period, a 10 nsec,  $1 \text{ cm}^{-1}$  bandwidth laser pulse from a Molelectron DL-200 dye laser pumped by a Molelectron UV-1000 nitrogen laser is passed through the ion cloud. Laser induced fluorescence is then monitored at right angles to the laser beam. A lens and mirror system directs some of the fluorescence through the wire mesh end electrodes to a cooled RCA 8575 photomultiplier tube.

In addition to fluorescence, scattered laser light may also reach the detection system. In order to minimize this background radiation, the laser beam is collimated to about 0.5 cm diameter with two lenses and directed through 0.5 meter arms (Fig. 2) containing light baffles on the entry and exit side of the trap.<sup>14</sup> In addition to the baffle system the 10 nsec laser pulse allows the use of gated detection techniques to reduce the effects of scattered laser light.

A signal from a trigger photodiode initiates a fluorescence detection gate. The initiation of the detection gate can be variably delayed with respect to the laser pulse, and its duration can be varied between 0.1 and 10  $\mu\text{sec}$ . The duration of the gate is primarily determined by the radiative lifetime of the species being investigated. The fluorescence detection gate and the signal from the PMT are sent to a gated single photon counting system which consists of an L.R.S. 621-BL discriminator and a 100 MHz counter (Ortec Model 770).

After the fluorescence detection, the experimental cycle is completed by pulsing the ions out of the trap to an electron multiplier. In order to get a consistent ion signal from cycle to cycle a high voltage pulse must be synchronized with the R.F. trapping potential and applied to the

bottom trap electrode. The resulting ion signal is measured by an L.R.S. 227-sg integrator and is used to normalize the fluorescence signal. The fluorescence signal is also normalized with respect to laser power which is measured by a photodiode and the gated integrator. The final signal gathered by the integrator is used to calibrate the laser wavelength. Calibration is accomplished with the use of the optogalvanic effect<sup>15</sup> in which the laser beam is directed into a hollow cathode discharge lamp containing neon. The fluorescence excitation spectrum is then calibrated with respect to Ne metastable transitions which are known throughout the visible region.

The timing of an experimental cycle is controlled by a series of logic circuits. The detection gates initiated by this timing circuitry are generated by Tektronix P.G. 501 pulse generators. The timing and gating logic are not shown in Fig. 2 in the interest of clarity. An on-line PDP-8f computer is responsible for the overall control of the experiment. At the end of an experimental cycle, the computer gathers the signals from the integrator and initiates a new cycle. After a predetermined number of cycles the computer retrieves the signal from the counter and advances the laser wavelength by a preset increment. Typically the signal is averaged over several hundred laser pulses before advancing the wavelength. The computer normalizes the data, stores them on a disk, and produces a hard copy graph of the spectrum.

The  $\text{CH}^+$  ( $\text{CD}^+$ ) spectra were produced under the following experimental conditions. The ions were created from  $\text{CH}_4$  ( $\text{CD}_4$ ) at a background pressure of  $10^{-5}$  Torr with an ionization period of 2.0 msec. The fluorescence detection gate was 1  $\mu\text{sec}$  in duration and was initiated 200 nsec after the laser pulse. The fluorescence signal was averaged over 500 laser pulses at each wavelength and the wavelength was advanced by 0.1  $\text{\AA}$  increments.

In the determination of radiative lifetimes, the experimental arrangement is modified somewhat. Control of the experimental timing is shifted from the computer to an internally controlled pulse cycle. The timing sequence is unchanged when operating in this mode, but the laser wavelength remains fixed, and the signal is collected continuously. The output signal from the PMT is fed into a discriminator and then into a Tracor Northern NS 575 digital signal averager with a Biomation time base.

This system provides a 10 nsec channel width which is suitable for the radiative decay rates encountered in the present studies. The Biomation time base is triggered by the pulse which initiates the detection gate in the normal mode of operation. The total width of the signal averager's time base in these studies was 1024 channels; i.e., 10.24  $\mu$ sec.

For the collection of frequency scanned spectra, the Molelectron UV-1000 nitrogen laser is used as a pump source for the dye laser because such lasers possess relatively high duty cycles. The fluctuations in laser power are corrected for on a shot to shot basis as discussed earlier. For measurements of fluorescence decay rates, however, it is desirable to maintain a steady laser power level throughout each determination. The frequency tripled output of a Quanta Ray Nd:YAG laser was found to vary in output power by only a few per cent and was used as the dye laser pump for all decay rate measurements.

For radiative decay measurements the dye laser is tuned into resonance with a strong transition in the vibronic band under study. The resulting fluorescence signal as a function of time is then accumulated in the signal averager for a period of several hundred thousand experimental cycles. The dye laser is then detuned from resonance, typically

by several  $\text{\AA}$ , and a background signal is subtracted for an equivalent time period. Data from the signal averager are then transferred to a PDP-8 computer for analysis. The experimental arrangement is schematically depicted in Fig. 3.

## RESULTS AND DISCUSSION

Laser induced fluorescence spectra were collected for the  $0 \leftarrow 0$  and  $2 \leftarrow 1$  bands of the  $A^1\Pi - X^1\Sigma^+$  system for both  $\text{CH}^+$  and  $\text{CD}^+$ . Representative portions of each band are reproduced in Fig's 4 and 5. Observed line frequencies are tabulated in Tables I, II and III. Because no new lines belonging to the  $2 \leftarrow 1$  band of  $\text{CH}^+$  were observed, we have omitted this band from the tables. Assignments for lines belonging to the  $\text{CH}^+$  band system were based upon the rotational constants of Douglas<sup>16</sup> which accurately reproduced low J components of each band but increasingly overestimated transition frequencies at higher J. It is clear that for a diatomic hydride such as  $\text{CH}^+$ , high J levels of a band system may not fit a Dunham expansion formula unless higher order correction terms are included (i.e.,  $H_v$  terms). Using the molecular constants of Douglas we calculated  $H_v$  constants for each band system but could not obtain adequate agreement between calculated and observed frequencies. Therefore, an unweighted least squares fit of all observed line frequencies was used to produce a new set of molecular constants given in Table IV. The  $\Lambda$  doubling constant,  $q_0$ , was found to identical to that deduced by Douglas and Morton:  $q_0 = 0.038 \text{ cm}^{-1}$ .

The rotational constants for  $\text{CD}^+$  obtained in emission studies by Antić-Jovanović *et al.*<sup>17</sup> were found to be adequate in reproducing low J components of each band for this isotopic species but, again, predicted

line frequencies too high for lines of increasing  $J$  (e.g.,  $5.8 \text{ cm}^{-1}$  too high for the  $0,0 R_{15}$  line). An unweighted least squares fit of all observed transition frequencies produced the set of molecular constants given in Table V.

The great difficulty encountered in attempting to fit high  $J$  components of each band with molecular constants derived using lower  $J$  terms is most likely due to the unusual nature of the  $A^1\Pi$  potential curve for both  $\text{CH}^+$  and  $\text{CD}^+$ . The nature of this potential is best understood if one examines the corresponding potential in the iso-electronic species,  $\text{BH}$ . This molecule has been the subject of careful emission studies<sup>18</sup> and has been determined to possess a barrier in the rotationless potential curve of the  $A^1\Pi$  state.<sup>19</sup> Early calculations<sup>20</sup> indicated that the  $A^1\Pi$  state arising from  $\text{B}(^2\text{P}) + \text{H}(^2\text{S})$  is initially repulsive in nature, but a strong interaction between this curve and an attractive curve arising from  $\text{B}(^2\text{D}) + \text{H}(^2\text{S})$  overcomes the repulsion and gives rise to the observed bound state.

While it might be expected that the  $A^1\Pi$  state of  $\text{CH}^+$  might exhibit similar behavior, the appearance of a potential maximum is by no means assured. The presence of the attractive charge-induced dipole force means that at large  $R$  values,  $A^1\Pi$  may well exhibit attractive behavior. If the interaction with the attractive curve arising from the  $\text{C}^+(^2\text{D}) + \text{H}(^2\text{S})$  asymptote becomes strong before the repulsive nature of the  $A^1\Pi$  curve overcomes the charge-induced dipole attraction, the result is a bound potential curve with unusual  $R$  dependence but no potential maximum. The calculations of Green *et al.*<sup>21</sup> suggest that, in fact, there is no actual barrier in the rotationless curve.

As is apparent upon examination of the spectra reproduced here, we have observed no laser induced fluorescence which is not attributable to

the particular ion under study. The present study covered the wavelength region from  $4130 \text{ \AA}$  to  $4400 \text{ \AA}$ . A thorough search throughout this wavelength region was conducted for any possible interfering species such as background neutral fluorescence or transitions originating in metastable levels of  $\text{CH}^+$  populated in the ion formation process. No such interference was found. The recent photodissociation studies of Cosby *et al.*<sup>22,23</sup> suggest that the  $^3\Pi$  state of  $\text{CH}^+$  ( $T_e \approx 9200 \text{ cm}^{-1}$ ) is, in fact, populated to some extent in the electron impact ionization of  $\text{CH}_4$ , although the relative amount of population in the singlet and triplet manifolds is difficult to estimate from the available data. If the analysis of Carre<sup>24</sup> is correct then transitions belonging to the  $^3\Sigma \leftarrow ^3\Pi$  system might be expected to appear strongly only below  $3700 \text{ \AA}$ , thus leaving the spectral regions under study here free from interference.

Several interesting features are apparent in the spectra presented here. Examination of the spectra reveals a linewidth noticeably larger than the bandwidth of the dye laser. The source of this broadening is the large Doppler profile of ions stored in a trap such as this. Recently,<sup>25</sup> a study of the spacial distribution of  $\text{Li}^+$  in a quadrupole trap similar to our own determined a line width consistent with an ion thermal temperature of 5000 K. Thus, for an ion of a similar charge to mass ratio, and for similar operating conditions it is reasonable to expect such a line broadening. We estimate an ion translational temperature of  $\sim 4000 \text{ K}$  for ions stored under the conditions described here.

A result of this large translational energy is that ions produced with a given rotational population distribution may be thermalized to a temperature much higher than room temperature. This may be done by introducing some inert gas to the vacuum chamber in addition to the

parent gas, but at a higher partial pressure, and allowing the ions to experience many high energy collisions. Using this approach it should be possible to collisionally populate high J levels in selected ions and to observe, by suitable means, rotational predissociation, thus providing accurate estimates of dissociation energies. Such information is generally lacking for molecular ions.

Another interesting feature which is evident in both spectra is the high rotational temperature of the ions even in the absence of such collisional effects. This stands in contrast to the apparently much cooler rotational distribution observed in emission studies. One may infer from published emission photographic plates and tabulations of observed lines a rotational temperature of 350 to 400 K for ions created in the  $A^1\Pi$  state, whereas, in the present study, rotational distributions corresponding to temperatures of 3000 K are seen for the  $X^1\Sigma^+$  state. This broad rotational distribution is not the result of high energy ion-neutral collisions involving  $CH^+(CD^+)$  of the type mentioned above as the experimental conditions under which these spectra were obtained provide a nearly collision free environment for the ions. Thus, this distribution reflects the initial product state distribution of  $CH^+(CD^+)$   $X^1\Sigma^+$  created in the electron impact fragmentation of methane (excepting possible radiative contributions from short lived electronic states). The cooler distributions characteristic of the emission studies are most likely the result of the many thermalizing collisions which may occur at the high pressures employed.

A comparison of the relative intensities of transitions originating in  $v'' = 0$  and  $v'' = 1$  also provides a measure of the degree of internal excitation. By scaling the observed transition intensity by the transition

probability an estimate of the relative vibrational populations can be made. For  $\text{CH}^+$  a convenient line for this comparison is the  $Q_9$  line which is clearly separated from other components in both bands. Using calculated oscillator strengths tabulated by Kusumoki and Ottinger<sup>26</sup> a vibrational temperature of  $\sim 5500$  K is obtained. This value is nearly a factor of two greater than the corresponding temperature derived earlier from the rotational distribution. Laser induced fluorescence spectra were also recorded for the  $0 \leftarrow 0$  band of this transition using  $\text{C}_2\text{H}_2$  as a source of  $\text{CH}^+$ . It was found that the apparent rotational and vibrational population distributions are essentially identical to those obtained using  $\text{CH}_4$  as a source.

Examination of the spectra obtained for  $\text{CD}^+$  yields similar conclusions. The rotational distribution is quite broad (as is expected for a much smaller  $B_0''$ ) with a characteristic temperature of  $\sim 3000$  K. The presence of transitions originating in  $v'' = 1$  is more pronounced in this case (as expected) permitting a more accurate determination of the molecular constants than for  $\text{CH}^+$ .

The feasibility of using the previously described experimental system to measure radiative lifetimes was tested by recording the radiative lifetimes of excited electronic states in several molecular ions for which reliable experimental data already exist. The systems chosen were the  $\text{N}_2^+ B^2\Sigma \rightarrow X^2\Sigma$  system with a  $v' = 0$  radiative lifetime of 60 nsec and the  $\text{CO}^+ A^2\Pi \rightarrow X^2\Sigma$  system with a  $v' = 2$  radiative lifetime of 3.25  $\mu\text{sec}$ . These two limits provide a sensitive test of the reliability of our approach for both short and long lifetimes. The results were in excellent agreement with accepted values.<sup>27-29</sup>

Direct measurements of the  $A^1\Pi$  radiative lifetime were made for the  $v' = 0$  level in both  $\text{CH}^+$  and  $\text{CD}^+$ . The results for  $\text{CH}^+$  are presented in

Fig. 6. The line used to pump this transition was the strong bandhead line consisting of the overlapping  $R_3$  and  $R_5$  members of the 0-0 band (see Fig. 4). The radiative lifetime determined in this study,  $\tau_0 = 815$  nsec, is larger than any previous experimental determination. This result is, however, in rather good agreement with the theoretical results of Yoshimine *et al.*<sup>10</sup> which predict a radiative lifetime for the  $A^1\Pi$  ( $v=0$ ) state of from 660 - 800 nsec. The range of presently accepted experimental values spans 250 nsec<sup>8</sup> to 630 nsec.<sup>9</sup> All previous attempts to record the radiative lifetime of this ion has relied upon some variation of the high frequency electron deflection technique described by Smith.<sup>5</sup> This method is potentially subject to error in several respects. High energy (several keV) electrons are used to create the excited  $CH^+$  from some parent neutral molecule. Such high energy electrons make any specific state selection in the ion impossible and almost certainly result in population cascading from highly excited electronic states of the ion. A second significant source of error which may manifest itself is the rapid spacial dissipation of ions from the effective viewing region due to the strongly repulsive ion-ion forces. Erman<sup>9</sup> has attempted to minimize the distortions of the measured decay curve due to the second effect by introducing low energy electrons to the ionization region, thus neutralizing some of the space charge due to the positive ions. In this respect, it is significant that the result be obtained,  $\tau_0 = 630$  nsec, is that in closest agreement with our own.

We measured the radiative lifetime for  $CD^+ A^1\Pi$  ( $v' = 0$ ) using the overlapping  $R_3$  and  $R_5$  lines (see Fig. 5) as a pumping level. The result obtained,  $820 \pm 50$  nsec, is slightly larger than that found for  $CH^+$  but the accompanying error is larger due to the weaker signal.

The oscillator strength for the (0,0) band of  $\text{CH}^+$  can be estimated by scaling the calculated value<sup>10</sup> ( $f_{00} = 6.45 \times 10^{-3}$ ) by the ratio of the calculated to the measured radiative lifetimes. The result is  $f_{00} = (5.8 \pm 0.2) \times 10^{-3}$ .

#### SUMMARY

These experiments have probed the ro-vibronic distribution of the ground electronic state of  $\text{CH}^+$  and  $\text{CD}^+$  fragment ions created by electron impact ionization of  $\text{CH}_4$  and  $\text{CD}_4$ . These ions are found to have substantial rotational and vibrational excitation, and many new transitions originating from high J states are observed. Essentially the same distributions are found whether methane or acetylene are used as parent gases. In addition, the radiative lifetime of the  $v = 0$  level of the  $\text{A}^1\Pi$  state was measured and found to be in good agreement with calculated values, but considerably longer than previously measured values. The technique described here should prove to have wide application to the study of small reactive ions.

We are grateful to the C. B. Moore group for the use of and assistance with the signal averaging equipment used in this work. The Nd:YAG laser was supplied by the San Francisco Laser Center supported by the National Science Foundation under Grant CHE79-16250. We thank A. Kung for assistance with this laser.

This research was supported by the U. S. Department of Energy, Office of Basic Energy Sciences Division of Chemical Sciences under Contract No. W-7405-Eng-48. J.S.W. acknowledges support as an Alfred P. Sloan Research Fellow.

## REFERENCES

1. A. E. Douglas and G. Herzberg, *Can. J. Res.* 20, 71 (1942).
2. W. S. Adams, *Ap. J.* 93, 11 (1941).
3. W. Klemperer and P. M. Solomon, *Ap. J.* 178, 389 (1972).
4. F. J. Grieman, B. H. Mahan and A. O'Keefe, *J. Chem. Phys.* 72, 4246 (1980).
5. W. H. Smith, *J. Chem. Phys.* 54, 1384 (1971).
6. R. Anderson, D. Wilcox and R. Sutherland, *Nuc. Inst. Meth.* 110, 167 (1973).
7. J. Brzozowski, N. Elander, P. Erman and M. Lyyra, *Ap. J.* 193, 741 (1974).
8. N. H. Brooks and W. H. Smith, *Ap. J.* 196, 307 (1974).
9. P. Erman, *Ap. J.* 213, L89 (1977).
10. M. Yoshimine, S. Green and P. Thaddeus, *Ap. J.* 183, 899 (1973).
11. P. H. Dawson and N. R. Whetton, *Dyn. Mass Spec.* 2, 1 (1971); P. H. Dawson, *Int. J. Mass Spec. Ion Phys.* 14, 317 (1974); P. H. Dawson and M. Meunier, *Int. J. Mass Spec. Ion Phys.* 29, 269 (1979); P. H. Dawson and C. Lambert, *J. Vac. Sci. Tech.* 12, 941 (1975).
12. M. Benilan and C. Audoin, *Int. J. Mass Spec. Ion Phys.* 11, 421 (1973).
13. H. G. Dehmelt, *Adv. Atomic and Mol. Phys.* 3, 53 (1967); 5, 109 (1969).
14. J. G. Pruett and R. N. Zare, *J. Chem. Phys.* 64, 1774 (1976).
15. D. S. King and P. K. Schenck, *Laser Focus*, March, 60 (1978).
16. A. E. Douglas and J. R. Morton, *Ap. J.* 131, 1 (1960).
17. A. Antić-Jovanović, V. Bojović, D. S. Pešić and S. Weniger, *J. Mol. Spec.* 75, 197 (1979).

18. G. M. Almy and R. B. Horsfall Jr., Phys. Rev. 51, 491 (1937).
  19. G. Herzberg and L. G. Mundie, J. Chem. Phys. 8, 263 (1940).
  20. A. C. Hurley, Proc. Roy. Soc. A261, 237 (1961).
  21. S. Green, P. S. Bagus, B. Liu, A. D. McLean, and M. Yoshimine, Phys. Rev. A 5, 1614 (1972).
  22. P. G. Cosby, H. Helm and J. T. Moseley, Ap. J. 235, 52 (1980).
  23. P. G. Cosby and H. Helm, Presented at Thirty Fifth Symposium on Molec. Spec., Columbus, Ohio, June 1980.
  24. M. Carre, Physica, 41, 63 (1969).
  25. R. D. Knight and M. H. Prior, J. Appl. Phys. 50, 3044 (1979).
  26. I. Kusunoki and Ch. Ottinger, J. Chem. Phys. 71, 4227 (1979).
  27. L. W. Dotchin, E. L. Chupp and D. J. Pegg, J. Chem. Phys. 59, 3960 (1973).
  28. V. E. Bondybey and T. A. Miller, J. Chem. Phys. 69, 3597 (1978).
  29. G. R. Mohlmann and F. J. DeHeer, Chem. Phys. Lett. 43, 170 (1976).
-

Table I. Observed line frequencies (in  $\text{cm}^{-1}$ )  
for the  $\text{CH}^+ \text{A}^1\Pi \leftarrow \text{X}^1\Sigma^+ (0,0)$  band

J	R branch	Q branch	P branch
0	23619.85 <sup>a</sup>	--	--
1	23637.71	23591.89	--
2	23650.48	23581.77	23536.26
3	23658.14	23566.56	23498.57
4	23660.52	23546.23	23455.87
5	23657.55	23520.70	23408.37
6	23649.10	23489.92	23355.9
7	23635.01	23453.76	23298.4
8	23615.1	23412.16	23235.8
9	23589.2	23365.0	23168.2
10	23557.1	23311.9	23095.3
11	23518.6	23253.3	23017.0
12	23473.5	23188.1	22933.2
13	23422.0	23117.4	22843.9
14	23362.8	23029.5	22748.4
15	23296.2	22955.0	22647.5
16	23222.2	22863.0	22540.0
17	23139.9	22763.8	
18	23049.1	22658.1	
19	22950.6	22544.2	
20	22842.0		
21	22724.5		

<sup>a</sup> Entries quoted to two decimal places are the more accurate values from Douglas and Herzberg<sup>1</sup>. Those with one are from this measurement. The two data sets were used as listed here in the least-squares reduction.

Table II. Observed line frequencies (in  $\text{cm}^{-1}$ )  
for the  $\text{CD}^+ \text{A}^1\Pi \leftarrow \text{X}^1\Sigma^+ (2,1)$  band

J	R branch	O branch	P branch
0	24105.67		
1	24112.90	24091.05	
2	24116.01	24083.28	--- <sup>b</sup>
3	24115.80	24071.90	24039.15
4	24111.49	24056.70	24013.15
5	24103.30	24037.65	23983.24
6	24091.05	24014.69	23949.84
7	24075.02	23987.85	23912.44
8	24054.90	23957.16	23871.31
9	24031.0	23922.42	23825.4
10	24003.6	23883.75	--- <sup>b</sup>
11	23972.1	23840.82	23724.4
12	23937.5	23793.8	23667.0
13	23897.1	23741.0	
14	23853.0	23681.0	
15	23802.2		
16	23753.0		
17	23687.9		

<sup>a</sup> Entries quoted to two decimal places are the more accurate values from Antić-Jovanović *et al.*<sup>17</sup> Those with one are from this measurement. The two data sets were used as listed here in the least-squares reduction.

<sup>b</sup> Missing entries were weak or overlapped and not resolved.

Table III. Observed line frequencies (in  $\text{cm}^{-1}$ )  
for the  $\text{CD}^+ \text{A}^1\Pi \leftarrow \text{X}^1\Sigma^+$  (0,0) band

J	R branch	Q branch	P branch
0	23760.03 <sup>a</sup>		
1	23769.83	23744.90	
2	23776.93	23739.48	23714.63
3	23781.35	23731.40	23694.20
4	23783.00	23720.62	23671.10
5	23782.02	23707.10	23645.35
6	23777.90	23690.86	23616.94
7	23771.10	23671.86	23585.96
8	23761.53	23650.05	23552.25
9	23748.90	23625.40	23516.0
10	23733.31	23597.88	23477.0
11	23714.65	23567.38	23435.8
12	23692.1	--- <sup>b</sup>	23390.3
13	23667.5	23497.8	23343.6
14	23639.4	23458.4	23292.8
15	23608.2	23416.2	23239.4
16	23573.5	23370.2	
17	--- <sup>b</sup>	23320.9	
18	23493.2	23269.1	
19	23448.0	23212.2	
20	23397.9		
21	23345.3		
22	23286.9		
23	23219.3		

<sup>a</sup>See footnote a to Table II.

<sup>b</sup>See footnote b to Table II.

Table IV. Molecular constants (in  $\text{cm}^{-1}$ ) for the  $\text{CH}^+$  (0,0) band

$\nu_{00}$	23596.81 (01)*
$B_0^{\text{RP}}$	11.4532 (37)
$B_0^{\text{Q}}$	11.4169 (41)
$D_0^{\text{RP}}$	0.002050 (9)
$D_0^{\text{Q}}$	0.002049 (11)
$B_0^{\text{''}}$	13.9303 (40)
$D_0^{\text{''}}$	0.001373 (11)

\* Numbers in parentheses represent a one standard deviation uncertainty in the last digits of each constant.

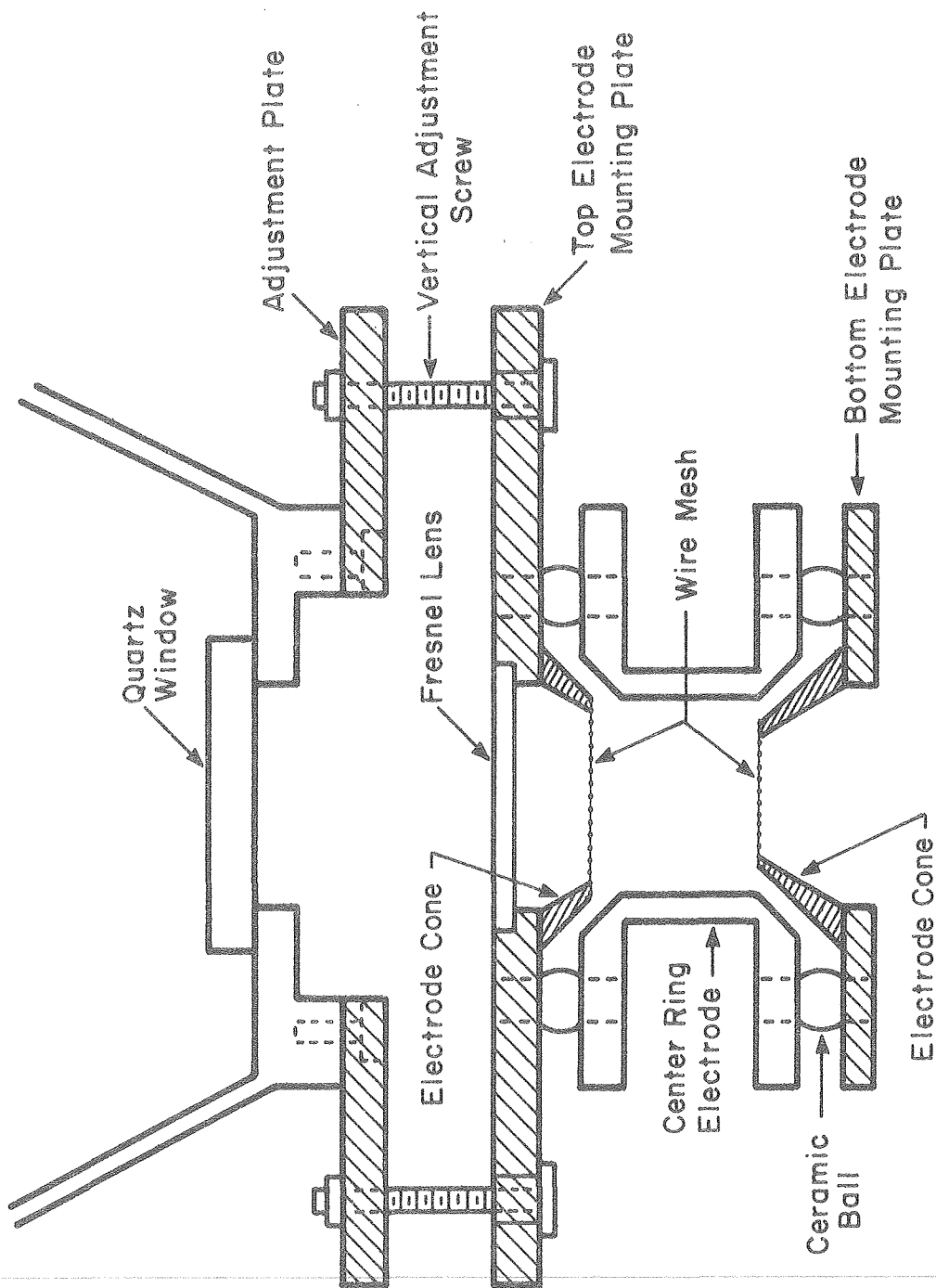
Table V. Molecular constants for the (0,0) and (2,1) bands of  $\text{CD}^+$ . Values in  $\text{cm}^{-1}$  and  $\text{\AA}$  units

	(0,0)	(2,1)
$\nu$	23747.71 (1)	24095.08 (1)
$B^{\text{RP}}$	6.285 (20)*	5.492 (44)
$B^{\text{Q}}$	6.280 (21)	5.479 (49)
$D^{\text{RP}}$	0.00108 (14)	0.00088 (48)
$D^{\text{Q}}$	0.00116 (16)	0.00071 (62)
$H^{\text{RP}}$	$1.12 (29) \times 10^{-6}$	$2.5 (1.5) \times 10^{-6}$
$H^{\text{Q}}$	$1.41 (37) \times 10^{-6}$	$1.2 (2.2) \times 10^{-6}$
$B'_e$		6.481 (30)
$\alpha'_e$		0.39 (3)
$R'_e$		1.228 (5)
$q$	0.016	0.014
$B''$	7.627 (20)	7.416 (46)
$D''$	0.00106 (15)	0.00125 (56)
$H''$	$1.55 (35) \times 10^{-6}$	$4.5 (2.0) \times 10^{-6}$
$B''_e$		7.733 (40)
$\alpha''_e$		0.21 (4)
$R''_e$		1.125 (4)

\* See footnote, Table IV.

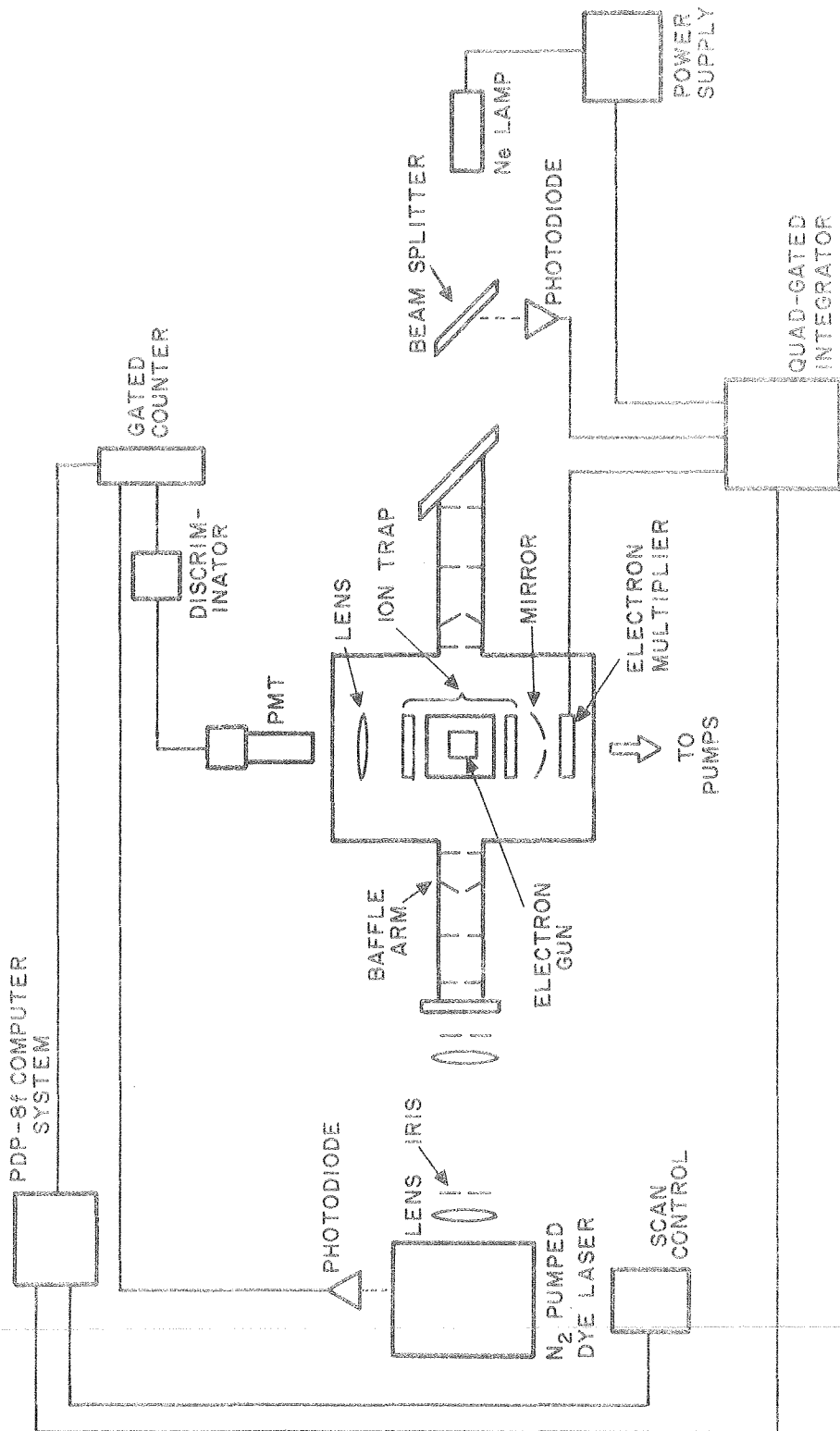
## FIGURE CAPTIONS

- Figure 1. Schematic representation depicting a vertical slice of the quadrupole ion trap used in the present study. A radio frequency voltage is applied to the center ring electrode while the top and bottom electrodes are maintained at ground potential. Ions, spacially confined to the enclosed region, possess a nearly Gaussian density distribution peaking at the center of the trap.
- Figure 2. Experimental arrangement used in the frequency scanning experiments. The depicted arrangement and timing sequence are discussed in the text.
- Figure 3. Experimental arrangement used to determine radiative lifetimes. The resulting signal trace is fed to a PDP-8 computer for data analysis.
- Figure 4. Representative portion of the spectrum obtained for the (0,0) band of the  $\text{CH}^+ \text{A}^1\Pi \leftarrow \text{X}^1\Sigma^+$  system. The  $\text{Q}_9$  line belonging to the (2,1) band of the same system is identified with an arrow in the lower portion of the figure. While other members of this band should be apparent in this wavelength region, overlap with members of the (0,0) band preclude their identification.
- Figure 5. Representative portions of the spectra obtained for the (0,0) and (2,1) bands of the  $\text{CD}^+ \text{A}^1\Pi \leftarrow \text{X}^1\Sigma^+$  system. The unobserved  $\text{P}_{10}$  line (denoted by an X) is buried in the (0,0) bandhead.
- Figure 6. Least squares fit to the data collected from the decay of the  $\text{A}^1\Pi$  ( $v'=0$ ) level of  $\text{CH}^+$ . The result,  $\tau = 815 \pm 25$  nsec, is the average of several such measurements.



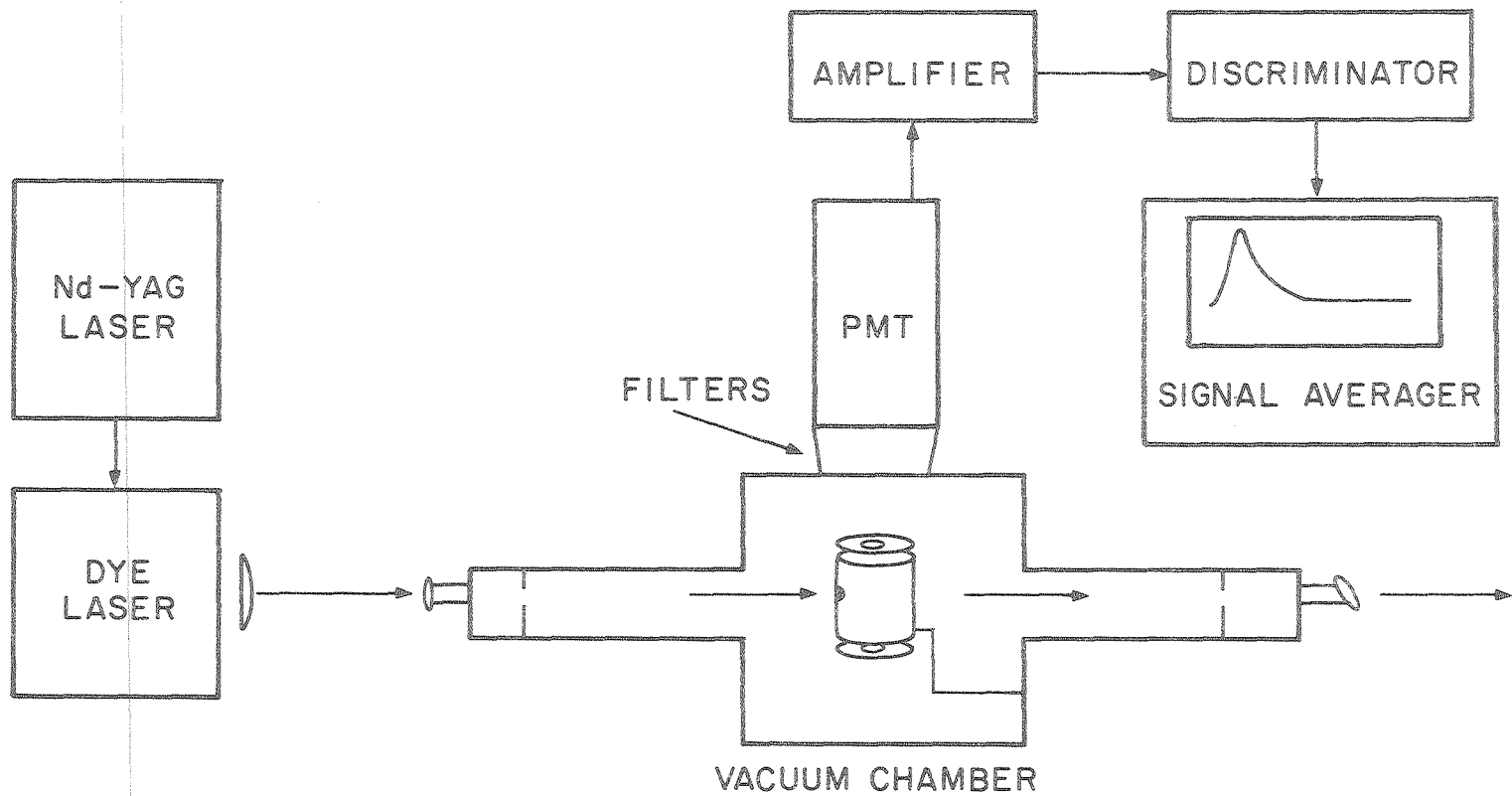
XBL 798-11079

Figure 1



XBL 807-10716 A

Figure 2



XBL 807-10712

Figure 3

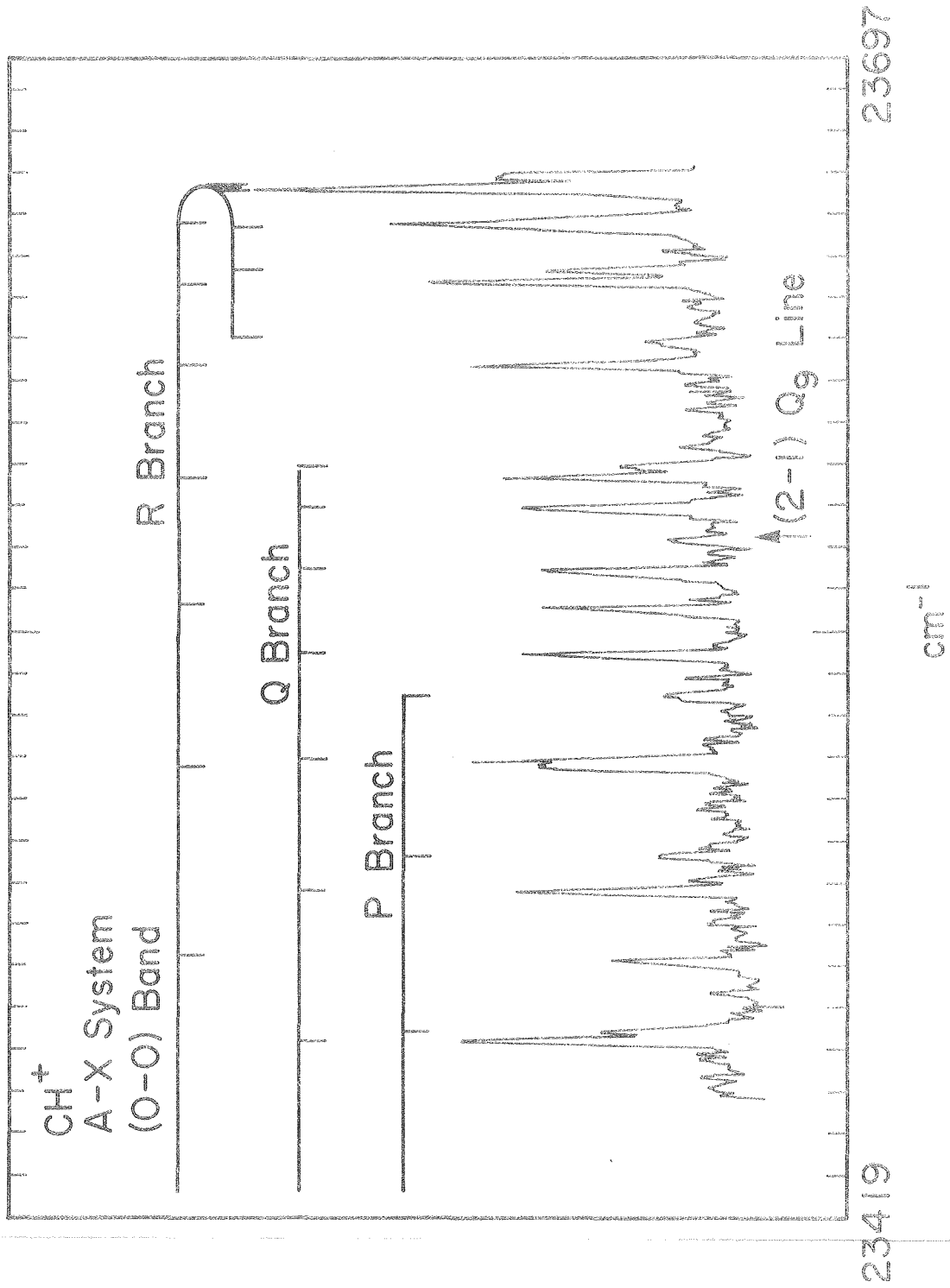
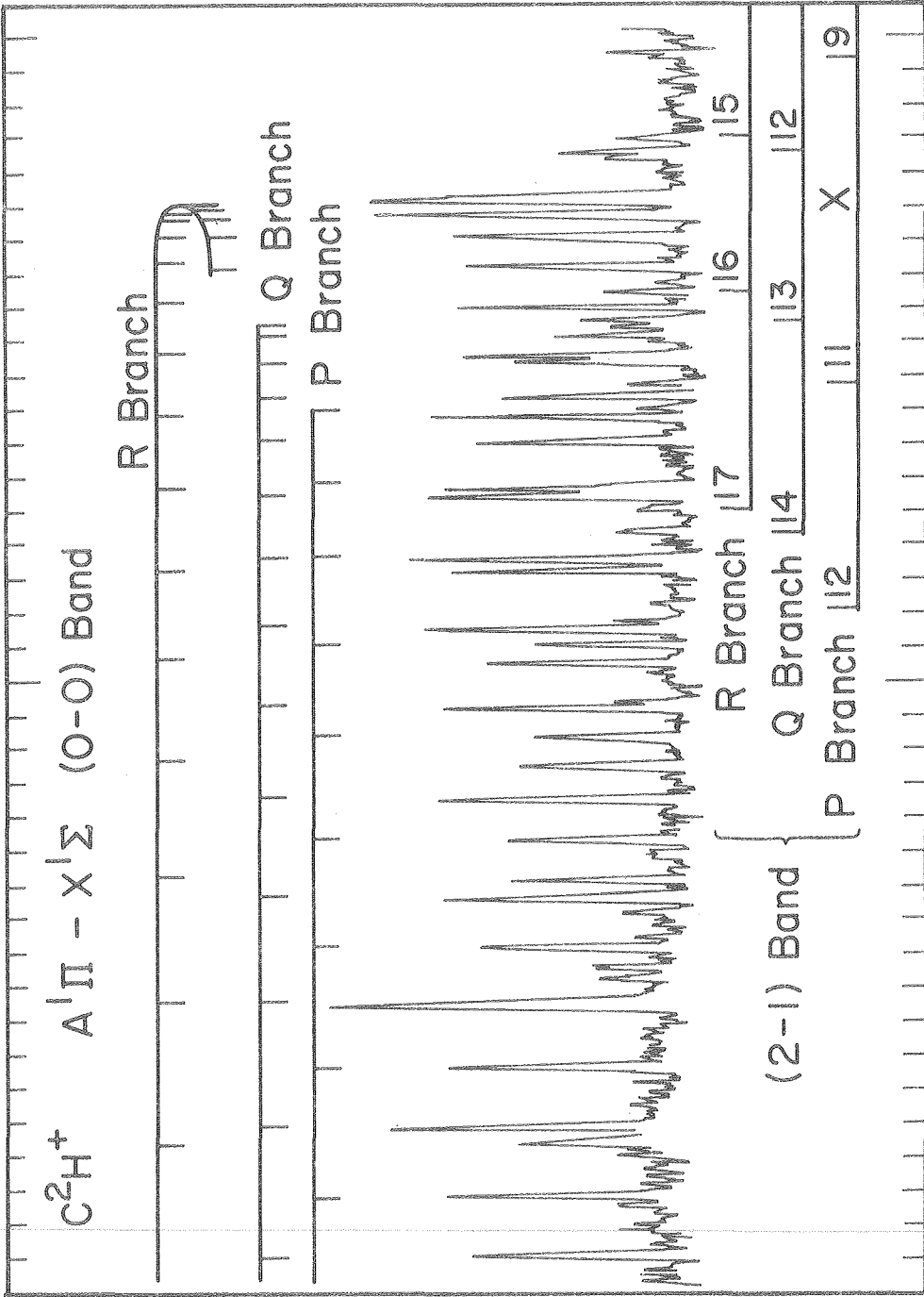


Figure 4

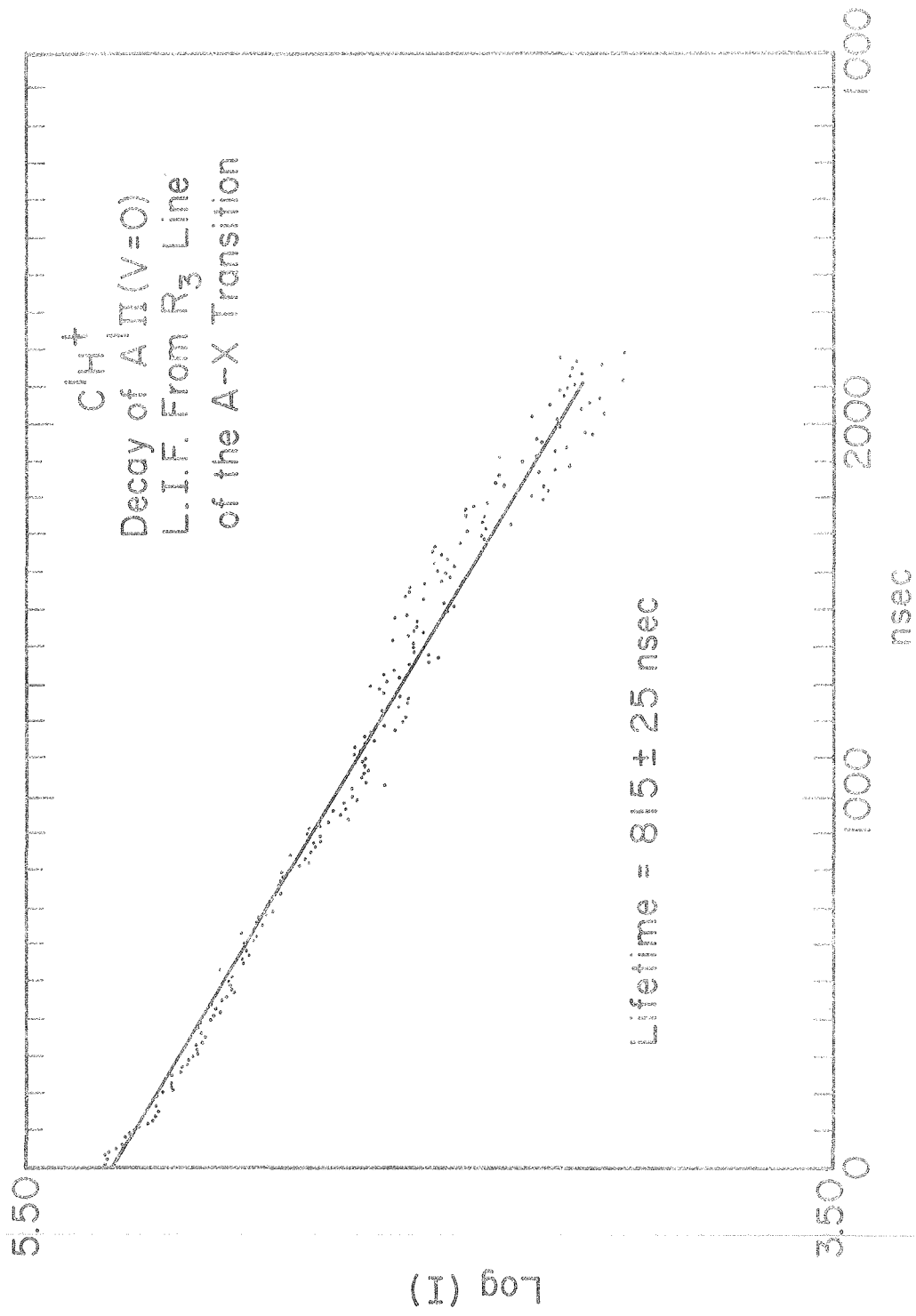
XBL 808-11411



23456 23824  
cm<sup>-1</sup>

XBL 808-11413

Figure 5



XBL 808-11410

Figure 6

